

# THESEUS Insights into ALP, Dark Photon and Sterile Neutrino Dark Matter

Charles Thorpe-Morgan<sup>1</sup>, Denys Malyshev<sup>1</sup>, Andrea Santangelo<sup>1</sup>,

Josef Jochum<sup>2</sup>, Barbara Jäger<sup>2</sup>, Manami Sasaki<sup>3</sup>, Sara Saeedi<sup>3</sup>

<sup>1</sup> *Institut für Astronomie und Astrophysik Tübingen,*

*Universität Tübingen, Sand 1, D-72076 Tübingen, Germany*

<sup>2</sup> *Eberhard Karls Universität Tübingen, 72076 Tübingen, Germany*

<sup>3</sup> *Remeis Observatory and ECAP, Universität Erlangen-Nürnberg, Sternwartstrasse 7, 96049 Bamberg, Germany*

Through a series of simulated observations, we investigate the capability of the instruments aboard the forthcoming *THESEUS* mission for the detection of a characteristic signal from decaying dark matter (DM) in the keV-MeV energy range. We focus our studies on three well studied Standard Model extensions hosting axion-like particles, dark photon, and sterile neutrino DM candidates. We show that, due to the sensitivity of *THESEUS*' X and Gamma Imaging Spectrometer (XGIS) instrument, existing constraints on dark matter parameters can be improved by a factor of up to around  $\sim 300$ , depending on the considered DM model and assuming a zero level of systematic uncertainty. We also show that even a minimal level of systematic uncertainty of 1% can impair potential constraints by one to two orders of magnitude. We argue that nonetheless, the constraints imposed by *THESEUS* will be substantially better than existing ones and will well complement the constraints of upcoming missions such as *eXTP* and *Athena*. Ultimately, the limits imposed by *THESEUS* and future missions will ensure a robust and thorough coverage of the parameter space for decaying DM models, enabling either a detection of dark matter or a significant improvement of relevant limits.

## I. INTRODUCTION

Dark matter (DM) remains one of the greatest obstacles to our understanding of cosmology. The presence of a universally pervading extra mass is clear and has been precisely measured ( $\Omega_{DM} = 0.2641 \pm 0.0002$  [1]); however, apart from its presence in the Universe, the nature and properties of dark matter remain elusive. The Standard Model (SM) is known not to host viable dark matter candidate particles, which has led to the consideration of various extensions to the SM that host potential dark matter candidates, see [2–4] for recent reviews.

A very general low energy extension of the SM is comprised of a “dark sector”, so called due to its extremely weak interaction with the SM. While such a sector can, in principle, host a variety of new particles providing natural DM candidates (see [5] for a review) and self-interactions, it can most easily be accessed via interactions between the dark and SM sectors. Such cross-sector interactions are often undertaken through a “mediator” – a particle with both, SM and dark sector, quantum numbers. Alternatively the SM particles can interact with the DM particles either directly (if they possess charge under the corresponding interaction) or through mixing. Some representative types of DM models are [6, 7]:

- models with (pseudo)scalar DM particles, e.g. axions and axion-like particles (ALPs);
- models with sterile neutrinos acting as DM particles;
- models with a vector DM particle (e.g. a dark photon (DP)).

In the following, we investigate three well studied cases of these models with massive DM candidates, which have the potential to comprise the majority of the observed dark matter. Namely, we will consider ALPs, sterile neutrinos and dark photons as dark matter candidates.

In these models a dark matter particle can decay, sequentially emitting photons. An axion or ALP  $a$  can decay into two photons  $a \rightarrow \gamma + \gamma$ . Sterile neutrino dark matter  $N$  can manifest itself via a two body decay:  $N \rightarrow \nu + \gamma$ , while dark photons  $V$  are subject to three-photon decay  $V \rightarrow 3\gamma$  (a preferable decay channel for  $m_V < m_e$  [3]).

The foremost consequence of such radiative decay channels would be the potential for a detectable signal originating from DM dominated astrophysical objects. The detection of such a signal would allow the indirect detection of dark matter decay events.

While, generally, any astrophysical object with a high DM concentration can be a target for such searches, one must consider additional astrophysical properties of the object to analyse its feasibility as the focus of such a search. For example, the high DM density and a low level of astrophysical background makes dwarf spheroidal galaxies (dSphs) advantageous targets for dark matter searches across a considerable section of the electromagnetic spectrum. However, dSphs are at most degree-scale targets, and such a small angular size does not allow for the full utilisation of the capabilities of broad field of view (FoV) instruments. Conversely, when considering wide FoV instruments, much wider objects with angular extensions of close to the whole sky (e.g. DM halo of the Milky Way) are preferable targets for these instruments.

Despite numerous searches, no clear evidence for any of the described dark matter candidates has been found so far. These searches have however allowed for parameters (mass and/or coupling strengths) to be significantly constrained for all candidates considered in this work.

The fundamental limit on the sterile neutrino mass  $m_N \gtrsim 1$  keV arises from the requirement that the phase space density of DM particles in the halos of dSphs may

not exceed the limits imposed by the uncertainty relation and the initial phase space density at the moment of production of DM in the Early Universe [8–11]. The mixing with active neutrinos is also constrained from above and below by the non-detection of a decay line in astrophysical observations and the exclusion of values that would lead to a discrepancy between observed and predicted abundances of light elements produced during Big Bang Nucleosynthesis [12–17].

The best limits on ALPs in different energy bands are based on observations of objects of totally different nature. These include: astrophysical observations (non-detection of a decay line in the  $\gamma$ -ray background) in the keV-MeV mass range; limits based on the evolution of horizontal branch stars (eV-keV masses); or direct detection experiment limits and astrophysical limits based on non-detection of ALP-photon conversion in certain magnetised astrophysical objects, see [3, 18] for reviews.

Dark photon parameters are subject to the constraints from non-observation of a spectral feature in the spectrum of galactic diffuse background (for masses  $m_V \gtrsim 10$  keV); stellar-evolution constraints (including the Sun, horizontal branch, and red giant stars [19]) for masses  $m_V \sim 10^{-6} - 10^4$  eV; cosmological and direct detection experiment limits at lower masses, see [3, 20] for reviews.

In what follows we study the capabilities of the forthcoming Transient High Energy Sky and Early Universe Surveyor (*THESEUS* [21–24]) mission to constrain parameters of keV-MeV mass scale dark matter focusing on the candidates described above.

*THESEUS* is a European mission concept<sup>1</sup> designed in response to the ESA call for medium-size mission (M5) within the Cosmic Vision Program<sup>2</sup>. The fundamental goals of the *THESEUS* mission are the study and detection of high energy transient phenomena, the study of the early universe and the epoch of re-ionisation, and “the hot and energetic universe”. These goals are planned to be achieved using the mission’s unique combination of instruments.

The *THESEUS* mission will host a total of three telescope arrays, covering a section of the infrared regime as well as the energy range of soft and hard X-rays. The proposed instrumental payload for *THESEUS* is:

–The Soft X-Ray Imager (SXI), an array of 4 lobster-eye telescope units with a quasi-square FoV covering the energy range of 0.3 – 5 keV with an effective area of  $A_{eff} \approx 1.9$  cm<sup>2</sup> at 1 keV and an energy resolution  $\sim 4\%$ . These will cover a total FoV of  $\sim 1$  sr with source location accuracy  $< 1 - 2$  arcminutes (for a full review of the instrument see [25]).

–The InfraRed Telescope (IRT), a single large (0.7 m) telescope that will be used for follow-up observations of

gamma-ray bursts. It will operate in the wavelength band 0.7 – 1.8  $\mu$ m and have a  $15' \times 15'$  FoV (for further specifications on the IRT see [26]).

–The X-Gamma Ray Imaging Spectrometer (XGIS) array, consisting of coded-mask cameras (with the total half-sensitive FoV comparable to that of the SXI) using monolithic X-gamma ray detectors based on bars of silicon diodes coupled with CsI crystal scintillator. XGIS will operate in the energy range of 2 keV – 20 MeV, which will be achieved using the two different detectors, referenced hereafter as XGIS-X and XGIS-S. The Silicon Drift Detector (SDD) will cover the energy range of 2–30 keV (XGIS-X) whereas the CsI scintillator will cover the range of 20 keV – 2 MeV (XGIS-S<sup>3</sup>). The effective areas and energy resolutions of XGIS-S are  $A_{eff}(300 \text{ keV}) \approx 1100$  cm<sup>2</sup> and energy resolution changing from  $\Delta E/E \sim 15\%$  at below 100 keV to  $\Delta E/E \sim 2\%$  at higher energies. The effective area and resolution of XGIS-X instrument are  $A_{eff}(10 \text{ keV}) \approx 500$  cm<sup>2</sup> and  $\Delta E/E \sim 1.5\%$ , see [27] for the full technical proposal for the XGIS.

Focusing on keV-MeV mass scale dark matter, we omitted the IRT from our further investigations. However, both the SXI and the XGIS, have large potential for the detection of DM decay given their very large FoVs (see e.g. discussion in [28]), thus the sensitivity simulations run by this study were performed for both these instruments.

Following this introduction, we present the methodology of our study of the capabilities of the forthcoming *THESEUS* mission to probe the parameter space of DM models with ALPs, sterile neutrinos and dark photons.

## II. SEARCH FOR DECAYING DM WITH *THESEUS*

The decay of massive ( $m_{DM}$ ) DM particles with an emission of  $\mu$  photons in each decay will result in the photon spectrum (as a function of photon energy  $E$ )

$$\frac{d\mathcal{F}}{d\Omega} \equiv \frac{dN}{dE dt dA d\Omega} = \frac{1}{4\pi} \cdot \frac{\mu J}{m_{DM}} \cdot \frac{d\Gamma(E)}{dE} \quad (1)$$

and a corresponding spectrum in the total field of view of the observing instrument:

$$\mathcal{F}_{FoV} = \int \frac{d\mathcal{F}}{d\Omega} d\Omega = \frac{\mu J_{FoV}}{4\pi m_{DM}} \cdot \frac{d\Gamma(E)}{dE}. \quad (2)$$

The  $J_{FoV}$  term in Eq. (2) is the total J-factor (DM mass column density) within the field of view and represents the astrophysical component of the dark matter signal. This is defined as the integral of the DM density

<sup>1</sup> selected by ESA on 2018 May 7 to enter an assessment phase study.

<sup>2</sup> See Cosmic Vision Program website

<sup>3</sup> Note, that due to the transparency of the XGIS coded mask at hard X-rays at  $E \gtrsim 150$  keV XGIS-X operates as a collimator.

over the field of view of the instrument and the line of sight (*l.o.s.*), i.e.

$$J_{FoV} \equiv \int J d\Omega = \int_{FoV} \int_{l.o.s.} \rho_{DM} d\ell d\Omega. \quad (3)$$

The  $\Gamma$  term in Eqs. (1)-(2) represents the radiative decay width – a model-dependent term given by the following three equations

$$\begin{aligned} \left. \frac{d\Gamma}{dE} \right|_{\nu MSM} &= \frac{9\alpha G_F^2}{256 \cdot 4\pi^4} \sin^2(2\theta) m_N^5 \delta(E - m_N/2); \quad (4) \\ \left. \frac{d\Gamma}{dE} \right|_{ALP} &= \frac{g_{a\gamma\gamma}^2 m_a^3}{64\pi\hbar} \delta(E - m_a/2); \\ \left. \frac{d\Gamma}{dE} \right|_{DP} &= \frac{2\kappa^2 \alpha_{QED}^4}{2^7 3^7 5^3 \pi^3 \hbar} \left( \frac{m_V}{m_e} \right)^8 \cdot f(x); \\ f(x) &= x \left( 1715 - 3105x + \frac{2919}{2} x^2 \right); x \equiv \frac{2E}{m_V}; x \in [0; 1], \end{aligned}$$

which correspond to each of the three models this study considers, see [3, 29–32]. Here  $m_N, m_a, m_V$  are the masses of the sterile neutrino, the ALP and the dark photon, respectively;  $\theta, g_{a\gamma\gamma}, \kappa$  are the sterile neutrino mixing angle, ALP-photon coupling strength and the DP kinetic mixing parameter, correspondingly;  $\alpha_{QED}$  and  $G_F$  stand for fine structure and Fermi constants.

Substituting the respective expressions of Eq. (4) into Eq. (2), using constants' values from [31], one obtains the expected signal for each model,

$$\begin{aligned} \mathcal{F}_{\nu MSM}(E) &\approx 10^{-7} \left( \frac{\sin^2(2\theta)}{10^{-16}} \right) \left( \frac{m_N}{10 \text{ keV}} \right)^4 \times \quad (5) \\ &\times \left( \frac{J_{FoV}}{10^{22} \text{ GeV/cm}^2} \right) \delta(E - m_N/2) \frac{\text{ph}}{\text{cm}^2 \text{ s keV}}; \\ \mathcal{F}_{ALP}(E) &\approx 1.2 \cdot 10^{-7} \left( \frac{m_a}{10 \text{ keV}} \right)^2 \left( \frac{g_{a\gamma\gamma}}{10^{-20} \text{ GeV}^{-1}} \right)^2 \\ &\times \left( \frac{J_{FoV}}{10^{22} \text{ GeV/cm}^2} \right) \delta(E - m_a/2) \frac{\text{ph}}{\text{cm}^2 \text{ s keV}}; \\ \mathcal{F}_{dph}(E) &\approx 4.08 \cdot 10^{-7} \left( \frac{\kappa}{10^{-10}} \right)^2 \left( \frac{m_V}{10 \text{ keV}} \right)^7 \cdot f \left( \frac{2E}{m_V} \right) \\ &\times \left( \frac{J_{FoV}}{10^{22} \text{ GeV/cm}^2} \right) \frac{\text{ph}}{\text{cm}^2 \text{ s keV}}; \end{aligned}$$

Here we inserted explicit numbers for the known fundamental constants [31] and parameters and accounted for a production of  $\mu = 1$  photon in sterile neutrino decays,  $\mu = 2$  photons for ALP decays and  $\mu = 3$  for three-photon dark photon decay.

The DM-decay signal for each model respectively will be comprised of the spectrum given by Eq. (5), and this signal is expected to be present in the real data on top of

astrophysical and instrumental backgrounds. Such a signal can be distinguished from the background due to its characteristic shape (a narrow line for  $\nu$ MSM or ALPs; a relatively broad spectral feature in the case of dark photons). The minimal detectable flux for a given instrument depends on several factors and may be estimated as:

$$F_{min} = \sigma \left( \sqrt{\frac{B\Delta E}{A_{eff} T \Omega_{FoV}}} + \alpha B \Delta E \right) \frac{\text{ph}}{\text{cm}^2 \text{ s sr}}. \quad (6)$$

Here,  $T$  is the exposure of observation (time duration for which data are taken), the instrument's effective area and energy resolution are given by  $A_{eff}(E)$  and  $\Delta E(E)$ , respectively, and the observed background (instrumental and astrophysical) is  $B(E)$  ph/(cm<sup>2</sup> s keV sr). The parameter  $\sigma$  stands for the significance level of the detection (e.g.  $\sigma = 2$  for  $2\sigma$  or  $\sim 95\%$  c.l. detection) and  $\alpha$  for the level of characteristic systematic uncertainty of the instrument. We note that for DM candidates producing a signal that is broader than the instrument's energy resolution, one must utilise the characteristic width of the signal, instead of  $\Delta E$ .

Using Eq. (6), the minimal detectable flux  $F_{min}(E)$  derived from the data can be compared to the expected dark matter decay signal  $\mathcal{F}_{DM}(E)$  given by Eq. (5) for the considered DM candidates. This allows the derivation of the range of dark matter parameters, which the instrument is capable of probing.

### A. Observational strategy

Any astrophysical object hosting a significant amount of dark matter can serve as a candidate for indirect searches for decaying dark matter. However, in order to maximise the instrument's potential for detection, the object must have an angular size in the sky comparable to the instrument's FoV. Conversely, the observation of an object with a much smaller angular size than the instrument's FoV will suffer from a deterioration of the J-factor (and thus resulting DM decay flux), as the integral  $J_{FoV} = \int J d\Omega$  vanishes beyond the characteristic size of the object. Therefore, neglecting to consider the relative size of the instrument's FoV can lead to an instrument's potential not fully being utilised. It is thus imperative to consider targets of a comparable angular size to the instrument's FoV.

In the context of indirect DM detection, the suite of X-ray instruments aboard *THESEUS* possesses uniquely broad fields of view ( $\sim 1$  sr) which pose the issue of being larger than the angular size of any extragalactic dark matter dominated object. Thus, with reference to the previous discussion of fields of view and object sizes, to fully utilise the capabilities of *THESEUS*, we propose to focus on indirect DM searches of local, Milky Way concentrations of dark matter with *THESEUS*' instruments. Additionally, in order to minimise the level of astrophysical background (e.g. Galactic Ridge X-ray emis-

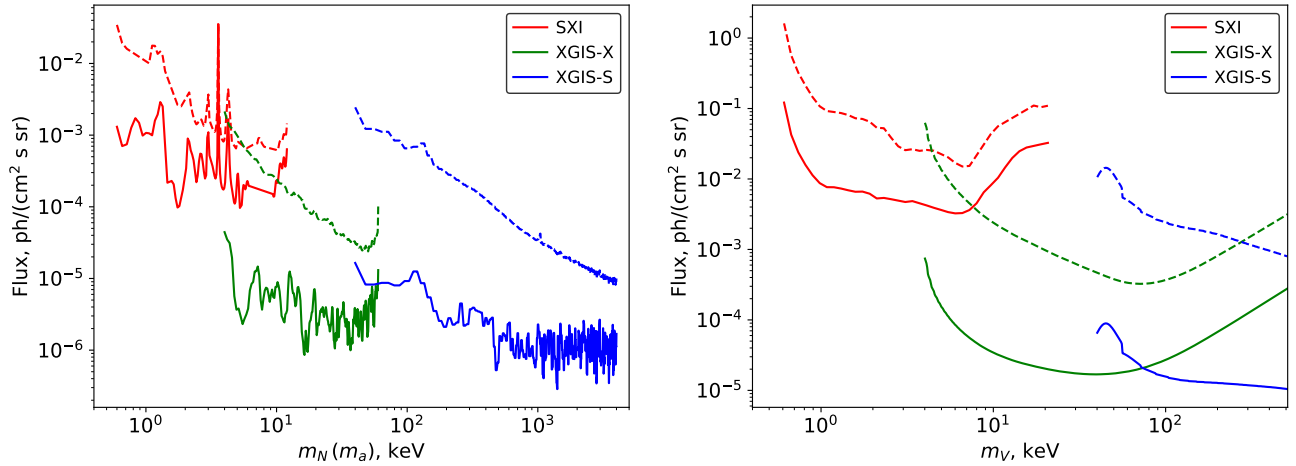


FIG. 1: The  $2\sigma$  limits on the sensitivity of the 1 Msec long observation with *THESEUS* instruments, to a narrow Gaussian line (*left panel*) and a spectral feature expected for a dark photon decay (*right panel*), see Eq. (5). The signal is assumed to be present in the whole FoV of the instrument. Dashed lines show the sensitivity of the instruments assuming a 1% systematic error in each respectively. Results are presented as functions of the mass of the DM particle.

sion, GRXE) we propose that the observations should be located away from the galactic plane. Namely, we propose the observations to be located at latitudes  $|b| > 20$  where GRXE contribution is minimal [33]. We note, that a similar strategy was proposed for the eXTP and several other broad-FoV missions [28, 34].

To estimate the J-factor in the FoV of *THESEUS*’ instruments, and, consequently, the strengths of the expected decaying DM signals (see Eq. (5)), we assume that the density of the dark matter in the Milky Way follows a Navarro-Frenk-White (NFW [35, 36]) profile:

$$\rho_{DM}(r) = \frac{\rho_0 r_0^3}{r(r + r_0)^2}, \quad (7)$$

with  $r_0 \approx 17.2$  kpc and  $\rho_0 \approx 7.9 \cdot 10^6 M_\odot/\text{kpc}^3$  [37].

The dark matter column density given by integrals in Eq. (3) was calculated numerically and the derived values of J-factors for proposed for observations regions are summarized in Tab. I. We would like to note that the results presented below do not depend directly on the considered DM profile, but rather on the J-factor (dark matter column density) value. These results can be re-scaled according to the  $J_{FoV}$  if another DM distribution model in the Milky Way is considered.

To access the minimal detectable flux level (Eq. 6) within *THESEUS* observations we estimated the expected background flux level from simulated 1 Msec-exposure blank sky observations with the *THESEUS*/SXI and XGIS instruments. The simulated data were obtained with the *fakeit* XSPEC (version: 12.10.1f) command, based on templates of blank sky observations provided by the *THESEUS* col-

laboration<sup>4</sup> (`sxi_bkg.pha`<sup>5</sup>, `XGIS-X_0deg_v7.bkg` and `XGIS-S_0deg_v7.bkg`) and corresponding response files. We note, that the provided templates are based on the estimations of both, instrumental and astrophysical backgrounds and thus any additional component(s) to model the astrophysical background were not included.

Our simulations revealed that the spectral shapes of the background are vastly different between the SXI and XGIS-S/X instruments. The background of the SXI can be adequately modelled by the sum of two models representing both the astrophysical and instrumental backgrounds. The model of the astrophysical background was selected to be a sum of a powerlaw and hot thermal plasma with the temperature  $\sim 0.2$  keV constituting contributions from cosmic X-ray background and galactic X-ray emission [38, 39]. The instrumental background was best modelled by the sum of a power-law (not convolved with the effective area) and a set of four narrow Gaussian lines. For this instrument we therefore propose the use of the common observational strategy whereby one searches for a decaying-DM spectral feature on top of an adequately modelled background. This method is widely used in decaying dark matter searches in various astrophysical objects, see [4] for a review.

On the other hand, the backgrounds of the two XGIS detectors are characterised by the presence of a large number of line-like and broad spectral features. We conclude that the XGIS’ background is significantly more complicated than SXI’s, and cannot be adequately modelled with any simple model. We thus propose the use of a different method for the XGIS, the “ON-OFF” observa-

<sup>4</sup> V7 templates dated May-July 2020; see [THESEUS webpage](#)

<sup>5</sup> Scaled by 17508, to account for template’s FoV (675 arcmin<sup>2</sup>).



tional strategy. This strategy requires the use of pairs of “ON” and “OFF” observations of comparable duration. We propose to locate the “ON” observations closer to the Galactic Center than “OFF” ones, so  $J_{FoV}^{ON} - J_{FoV}^{OFF} > 0$ . The estimations for  $J_{FoV}^{ON}$  and  $J_{FoV}^{OFF}$  for the sample “ON” and “OFF” observations are summarized in Tab. I.

We acknowledge the possibility of variation of the shape of the astrophysical (instrumental) background across the FoV (detector) of the instrument as well as possibility of variations of astrophysical background between “ON” and “OFF” regions. In the absence of detailed studies characterising such variations for the *THESEUS* instrument, we propose to estimate the impact of this effect by introducing a systematic uncertainty on *THESEUS* spectra. Other sources of uncertainty include an imperfect modelling of the instrumental background and an imperfect knowledge of the instrument’s response and effective area. Below, we present all results for the case of an absence of systematic uncertainty and compare them to the results in which a 1% systematic uncertainty was introduced<sup>6</sup>. In order to replicate the effects of systematic uncertainty, we introduced a new **STAT.ERR** column to the simulated spectral files which, in addition to the standard Gaussian error, included a value proportional to the total counts in each channel.

## B. Results

Following the previously outlined methodology for simulating observations in both of *THESEUS*’s instruments, we conducted a search for a dark matter decay signal with a spectral shape (for each respective model) given by Eq. (5) and originating from the whole FoV. We calculated  $2\sigma$  upper limits on the normalisation of the signal, allowing us to derive the sensitivities of each of *THESEUS*’ instruments to the parameters of the DM particle in the corresponding model. The  $2\sigma$  ( $\sim 95\%$  confidence level) limits on flux<sup>7</sup> from 1 Msec long observation of Milky Way halo are shown with solid red, green and blue curves, for the SXI, XGIS-S and XGIS-X instruments respectively, in Fig. 1. The left and right panels show the results for a narrow Gaussian line signal (sterile neutrino and ALP decay cases) and a broader spectral feature expected from a dark photon decay. Limits from observations where a 1% systematic uncertainty was introduced to each instrument are shown with dashed lines.

The displayed limits illustrate that the sensitivity of each of *THESEUS*’ instruments to a DM decay signal is detrimentally affected by the effect of poorly controlled systematics for all of the types of DM particles consid-

Observation	FoV deg <sup>2</sup>	Galactic coordinate centre	$J_{FoV}$ GeV/cm <sup>2</sup>
SXI Blank Sky	$\sim 104^\circ \times 31^\circ$	(110, 50)	$1 \times 10^{22}$
XGIS Blank Sky	$\sim 104^\circ \times 31^\circ$	On (0, 50) Off (110, 50)	$2 \times 10^{22}$ $1 \times 10^{22}$

TABLE I: Parameters of the simulated observations from blank sky readings. The FoV is assumed to be parallel to the galactic plane and roughly corresponds to the sky area at the border of which the effective area is 50% of the on-axis one, see [27]. Galactic coordinates show the coordinates of the FoV center in which the J-factor was calculated and the observation simulated (see text for details).

ered. For a narrow line signal (sterile neutrino or ALP dark matter candidates) the SXI will suffer from worsening of its limits by a factor of  $\sim 10$ , whereas the XGIS is significantly more affected, seeing a reduction by a factor of  $\sim 100$  in its sensitivity in both detectors. We therefore conclude that, despite the promising sensitivities of each instrument, instrumental systematics can be a significant obstacle and severely impair the ability of each instrument if not controlled.

For each of the considered DM models (ALPs, sterile neutrino and dark photons), we convert the obtained flux limits to the limits on the parameters of DM particles, see Eq. (5) and Figs. 2-3, and compare the obtained limits to other limits presented in the literature.

For the sterile neutrino we compared limits derived by this study to the existing observational X-ray and  $\gamma$ -ray constraints (see [4] for a review). We also display, for comparison, the expected limits from 1 Msec-long Segue I dSph observations by the forthcoming *Athena* mission [40] given a zero level of systematic uncertainty. The limits based on the phase space density arguments for the DM in dSphs [8–11] and otherwise incorrect abundance of sterile neutrinos produced in the Early Universe [41, 42] are shown as gray shaded regions. Model dependent limits based on parameter values that are inconsistent with the observed abundances of light elements produced during Big Bang Nucleosynthesis [12–16] (see, however, [17]) are shown as a gray hatched region.

The limits on ALPs were compared to the existing limits in the keV band based on the non-detection of a line-like feature in the spectrum of diffuse gamma-ray background in the keV-MeV band [18, 43]. The limits on dark photons, on the other hand, are compared to the stellar evolution-based limits (the Sun limits in longitudinal and transverse channels; the limits from horizontal branch and red giant stars’ evolution [19]) and the limits from the diffuse gamma-ray background, see [3, 20] for a review.

<sup>6</sup> Characteristic for *XMM-Newton* value, see [EPIC Calibration Status document](#)

<sup>7</sup> Corresponding upper limits on the normalization were calculated with **error 4.0** XSPEC command.

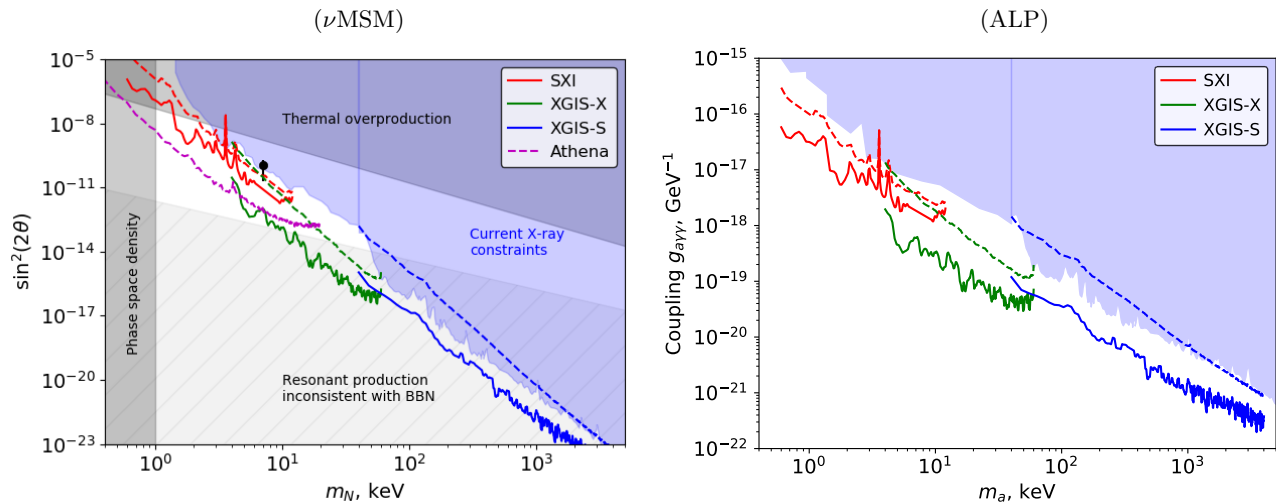


FIG. 2: The sensitivity of the instruments aboard *THESEUS* to the parameters of sterile neutrino and ALP dark matter. All limits correspond to the  $2\sigma$  values of the flux obtained from 1 Msec simulated observations of the Milky Way’s DM halo, see Tab. I for the details. On all panels red, green and blue solid curves present sensitivity limits for the SXI, XGIS-X and XGIS-S instruments, respectively, in case of absence of systematic uncertainties. Dashed curves illustrate similar limits for 1% systematics present in the data. Shaded regions present current exclusions adopted from [3, 4, 8–16, 18–20, 43]. *Left panel*: *THESEUS* sensitivity for the sterile neutrino ( $\nu$ MSM) DM. The Magenta curve illustrates limits reachable for Athena [40]. The black point represents the parameter point corresponding to the tentative detection of an  $\sim 3.55$  keV line in certain DM-dominated objects (see [44],[45] and [4] for a recent review). *Right panel*: Sensitivity limits for ALP dark matter, see text for details.

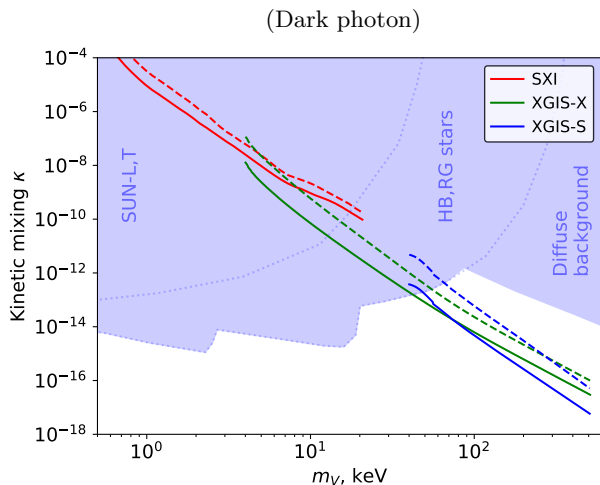


FIG. 3: The sensitivity of the instruments aboard *THESEUS* to the parameters of dark photon dark matter, see caption of Fig. 2 for designations and text for details.

### III. DISCUSSION AND CONCLUSIONS

This study has investigated the sensitivity of the proposed X-ray telescope arrays aboard the upcoming *THESEUS* mission to decaying dark matter signals from DM models with ALPs, sterile neutrinos and dark photons. Our results demonstrate that *THESEUS* has the potential to impose significantly better limits than the current

generation of instruments. The use of 1 Msec long *THESEUS* observations of blank sky regions has the potential to improve existing X-ray constraints on the parameters of dark matter, by a factor of up to  $\sim 300$ , within the keV-MeV dark matter particle mass range, see Fig. 2 and Fig. 3.

Regions proposed for observations are located at significant angular distance from the Galactic Center. This allows the minimisation of uncertainties connected to the knowledge of the exact shape of the dark matter profile and excludes the presence of strong astrophysical backgrounds. In case the *THESEUS* mission is approved with reduced specifications<sup>8</sup>, the relocation of observational regions closer to the Galactic Center can compensate (within a factor of  $\sim 2$ ) the subsequent decrease in the expected dark matter signal.

We also show that the XGIS has the potential to completely explore the sterile neutrino parameter space in the mass range  $m_N \sim 15 - 150$  keV (see Fig. 2, left panel), assuming a marginally possible 0% level of systematic uncertainty.

We assert that the effect of systematics on *THESEUS*’ instruments will be severely detrimental to their sensitivity to all types of decaying DM. We have shown a level of systematics at 1% can considerably worsen the constraints that can be achieved by both instruments, with

<sup>8</sup> See recent updates on [THESEUS mission website](#)

the limits imposed by the SXI and XGIS falling by up to factors of  $\sim 10$  and  $\sim 100$  respectively for all considered DM models. At these levels of systematic uncertainty, while the XGIS will remain able to probe new areas of the parameter space, the SXI's limits may, in certain ranges, be worse than the existing limits in this energy band. To summarise, only full control of the systematics in these instruments would make them a formidable addition in the search for DM.

The tentative detection of a 3.55 keV line in some DM-dominated objects [44, 45] is still actively being discussed in the field (see [4] for a recent review). Such a signal was originally proposed to originate from the decay of sterile neutrino with the mass  $m_N \sim 7$  keV and a mixing angle of  $(\sin^2(2\theta) \sim 2 \cdot 10^{-11})$ . The corresponding range of mixing angles discussed in the literature is denoted by the black point with error-bars in Fig. 2. We mention that the constraints displayed in Fig. 2 for a 0% systematic uncertainty (left panel) indicate also that *THESEUS* will be sensitive enough to exclude or detect this line, at a  $\gtrsim 7\sigma$  level ( $\sim 3\sigma$  level if 1% systematics is present). The strength of such a line could be compared to other DM-dominated objects or along the sky in order to correlate its intensity with the known  $J_{Fov}$  value, and thus draw conclusions on its possible DM-decay origin.

We would further like to note that several other mod-

els were proposed to explain the observed 3.55 keV signal. These models include scalar [46] and pseudo-scalar, ALP [47, 48] dark matter. We argue that the (non)detection of such a line by *THESEUS* can provide significant constraints on the parameters of these models.

The *THESEUS* mission, as well as its numerous scientific objectives, will play an essential part in high energy studies over the next decade. Its overlap with other planned missions such as eXTP and Athena provides prime potential for the complementary study of the decaying DM's parameter space using the above mentioned next generation satellites, among many others. The use of these instruments in conjunction with one-another has the potential to impose tighter limits on DM candidates than ever before and significantly decrease their unexplored parameter space.

We conclude that *THESEUS*, alongside well controlled systematics, has the potential to either detect decaying dark matter, or to impose some of the strongest constraints on its properties among its generation of satellites.

*Acknowledgements* The authors acknowledge support by the state of Baden-Württemberg through bwHPC. This work was supported by DFG through the grant MA 7807/2-1.

- 
- [1] Planck Collaboration, N. Aghanim, Y. Akrami, M. Ashdown, J. Aumont, C. Baccigalupi, M. Ballardini, A. J. Banday, R. B. Barreiro, N. Bartolo, et al., arXiv e-prints arXiv:1807.06209 (2018), 1807.06209.
  - [2] A. Boyarsky, D. Iakubovskyi, and O. Ruchayskiy, *Physics of the Dark Universe* **1**, 136 (2012), 1306.4954.
  - [3] M. Pospelov, A. Ritz, and M. Voloshin, *Phys. Rev. D* **78**, 115012 (2008), 0807.3279.
  - [4] A. Boyarsky, M. Drewes, T. Lasserre, S. Mertens, and O. Ruchayskiy, *Progress in Particle and Nuclear Physics* **104**, 1 (2019), 1807.07938.
  - [5] M. Battaglieri, A. Belloni, A. Chou, P. Cushman, B. Echenard, R. Essig, J. Estrada, J. L. Feng, B. Flaugher, P. J. Fox, et al., arXiv e-prints arXiv:1707.04591 (2017), 1707.04591.
  - [6] R. Essig, J. A. Jaros, W. Wester, P. Hansson Adrian, S. Andreas, T. Averett, O. Baker, B. Batell, M. Battaglieri, J. Beacham, et al., arXiv e-prints arXiv:1311.0029 (2013), 1311.0029.
  - [7] M. Raggi and V. Kozhuharov, *Nuovo Cimento Rivista Serie* **38**, 449 (2015).
  - [8] S. Tremaine and J. E. Gunn, *Physical Review Letters* **42**, 407 (1979).
  - [9] A. Boyarsky, O. Ruchayskiy, and D. Iakubovskyi, *J. Cosmology Astropart. Phys.* **3**, 005 (2009), 0808.3902.
  - [10] D. Gorbunov, A. Khmelnitsky, and V. Rubakov, *J. Cosmology Astropart. Phys.* **10**, 041 (2008), 0808.3910.
  - [11] D. Savchenko and A. Rudakovskiy, *MNRAS* **487**, 5711 (2019), 1903.01862.
  - [12] X. Shi and G. M. Fuller, *Phys. Rev. Lett.* **82**, 2832 (1999), astro-ph/9810076.
  - [13] P. D. Serpico and G. G. Raffelt, *Phys. Rev. D* **71**, 127301 (2005), astro-ph/0506162.
  - [14] M. Shaposhnikov, *Journal of High Energy Physics* **2008**, 008 (2008), 0804.4542.
  - [15] M. Laine and M. Shaposhnikov, *J. Cosmology Astropart. Phys.* **2008**, 031 (2008), 0804.4543.
  - [16] L. Canetti, M. Drewes, T. Frossard, and M. Shaposhnikov, *Phys. Rev. D* **87**, 093006 (2013), 1208.4607.
  - [17] A. Kusenko, *Phys. Rev. Lett.* **97**, 241301 (2006), hep-ph/0609081.
  - [18] P. W. Graham and S. Rajendran, *Phys. Rev. D* **88**, 035023 (2013), 1306.6088.
  - [19] J. Redondo and G. Raffelt, *J. Cosmology Astropart. Phys.* **2013**, 034 (2013), 1305.2920.
  - [20] M. Fabbrihesi, E. Gabrielli, and G. Lanfranchi, arXiv e-prints arXiv:2005.01515 (2020), 2005.01515.
  - [21] L. Amati, P. O'Brien, D. Gtz, E. Bozzo, C. Tenzer, F. Frontera, G. Ghirlanda, C. Labanti, J. Osborne, G. Stratta, et al., *Advances in Space Research* **62**, 191244 (2018), ISSN 0273-1177, URL <http://dx.doi.org/10.1016/j.asr.2018.03.010>.
  - [22] G. Stratta, R. Ciolfi, L. Amati, E. Bozzo, G. Ghirlanda, E. Maiorano, L. Nicastro, A. Rossi, S. Vinciguerra, F. Frontera, et al., *Advances in Space Research* **62**, 662682 (2018), ISSN 0273-1177, URL <http://dx.doi.org/10.1016/j.asr.2018.04.013>.
  - [23] G. Stratta, L. Amati, R. Ciolfi, and S. Vinciguerra, *The-seus in the era of multi-messenger astronomy* (2018), 1802.01677.
  - [24] N. R. Tanvir, *Theseus and the high redshift universe* (2018), 1802.01678.

- [25] P. O’Brien, E. Bozzo, R. Willingale, I. Hutchinson, J. Osborne, L. Amati, and D. Götz, *Mem. Soc. Astron. Italiana* **89**, 130 (2018), 1802.01675.
- [26] D. Götz, O. Boulade, B. Cordier, E. Le Floch, F. Pinsard, J. Amiaux, T. Turrette, S. Basa, S. Vergani, J. L. Atteia, et al., *Mem. Soc. Astron. Italiana* **89**, 148 (2018), 1802.01676.
- [27] R. Campana, F. Fuschino, C. Labanti, L. Amati, S. Mereghetti, M. Fiorini, F. Frontera, G. Baldazzi, P. Bellutti, G. Borghi, et al., *Mem. Soc. Astron. Italiana* **89**, 137 (2018), 1802.01674.
- [28] D. Zhong, M. Valli, and K. N. Abazajian, *arXiv e-prints arXiv:2003.00148* (2020), 2003.00148.
- [29] P. B. Pal and L. Wolfenstein, *Phys. Rev. D* **25**, 766 (1982).
- [30] V. Barger, R. J. N. Phillips, and S. Sarkar, *Physics Letters B* **352**, 365 (1995), hep-ph/9503295.
- [31] M. Tanabashi et al. (Particle Data Group), *Phys. Rev. D* **98**, 030001 (2018).
- [32] H. An, M. Pospelov, J. Pradler, and A. Ritz, *Physics Letters B* **747**, 331 (2015), 1412.8378.
- [33] R. Krivonos, M. Revnivtsev, E. Churazov, S. Sazonov, S. Grebenev, and R. Sunyaev, *A&A* **463**, 957 (2007), astro-ph/0605420.
- [34] D. Malyshev, C. Thorpe-Morgan, A. Santangelo, J. Jochum, and S.-N. Zhang, *Phys. Rev. D* **101**, 123009 (2020), 2001.07014, URL <https://link.aps.org/doi/10.1103/PhysRevD.101.123009>.
- [35] J. F. Navarro, C. S. Frenk, and S. D. M. White, *ApJ* **462**, 563 (1996), astro-ph/9508025.
- [36] J. F. Navarro, C. S. Frenk, and S. D. M. White, *ApJ* **490**, 493 (1997), astro-ph/9611107.
- [37] M. Cautun, A. Benitez-Llambay, A. J. Deason, C. S. Frenk, A. Fattahi, F. A. Gmez, R. J. J. Grand, K. A. Oman, J. F. Navarro, and C. M. Simpson, *The milky way total mass profile as inferred from gaia dr2* (2019), 1911.04557.
- [38] D. McCammon, R. Almy, E. Apodaca, W. Bergmann Tiest, W. Cui, S. Deiker, M. Galeazzi, M. Juda, A. Lesser, T. Mihara, et al., *ApJ* **576**, 188 (2002), astro-ph/0205012.
- [39] A. De Luca and S. Molendi, *A&A* **419**, 837 (2004), astro-ph/0311538.
- [40] A. Neronov and D. Malyshev, *Phys. Rev. D* **93**, 063518 (2016), 1509.02758.
- [41] S. Dodelson and L. M. Widrow, *Physical Review Letters* **72**, 17 (1994), hep-ph/9303287.
- [42] T. Asaka, M. Shaposhnikov, and M. Laine, *Journal of High Energy Physics* **1**, 091 (2007), hep-ph/0612182.
- [43] A. Boyarsky, D. Malyshev, A. Neronov, and O. Ruchayskiy, *MNRAS* **387**, 1345 (2008), 0710.4922.
- [44] A. Boyarsky, O. Ruchayskiy, D. Iakubovskiy, and J. Franse, *Physical Review Letters* **113**, 251301 (2014), 1402.4119.
- [45] E. Bulbul, M. Markevitch, A. Foster, R. K. Smith, M. Loewenstein, and S. W. Randall, *ApJ* **789**, 13 (2014), 1402.2301.
- [46] K. S. Babu and R. N. Mohapatra, *Phys. Rev. D* **89**, 115011 (2014), 1404.2220.
- [47] M. Cicoli, J. P. Conlon, M. C. D. Marsh, and M. Rummel, *Phys. Rev. D* **90**, 023540 (2014), 1403.2370.
- [48] J. P. Conlon and F. V. Day, *J. Cosmology Astropart. Phys.* **2014**, 033 (2014), 1404.7741.